**Sentinel node restoration by vascularized lymph node transfer in mice**

Running head: VLNT for sentinel node

Erika G. Kusajima, PhD[1]; Yuhei Yamamoto, PhD[1]; Kosuke Ishikawa, PhD[1]; Takahiro Miura, PhD[1]; Emi Funayama, PhD[1]; Masayuki Osawa, PhD[1]; Ryo Takagi, PhD[2]; and Taku Maeda, PhD[1]

[1]Department of Plastic and Reconstructive Surgery, Faculty of Medicine and Graduate School of Medicine, Hokkaido University, Sapporo, Hokkaido, Japan;

Corresponding author: Taku Maeda, PhD
Department of Plastic and Reconstructive Surgery, Faculty of Medicine and Graduate School of Medicine, Hokkaido University, Kita 15, Nishi 7, Kita-ku, Sapporo, Hokkaido 060-8638, Japan
Email: takumaeda1105@yellow.plala.or.jp

**Acknowledgments**

The authors thank Dr. Toshihiko Hayashi (PhD, MD, DDS, Department of Plastic and Reconstructive Surgery, Asahikawa Medical University, Japan) and Dr. Naoki Murao (PhD, MD, Department of Plastic and Reconstructive Surgery, Tonan Hospital, Japan) for their assistance throughout this study.

**Funding**

This study received no funding.

## Conflicts of interest

The authors declare no conflicts of interest.

## Ethical approval

All experiments were approved by the Institutional Animal Care and Use Committee at Hokkaido University and conducted in accordance with the Guidelines for the Care and Use of Laboratory Animals.

**Abstract**

***Background:*** Recent reports have indicated that vascularized lymph node transfer (VLNT) may improve the impaired immunity in lymphedema but there has been no report concerning anti-cancer immunity. In the early tumor immune response, dendritic cells (DCs) participate in tumor recognition and antigen presentation in local lymphatics. Here, we investigated the impact of VLNT on DC dynamics against cancer in mouse models.

***Methods:*** Forty-seven 8-week-old C57BL/6N male mice were divided into three surgical groups: a VLNT model in which a vascularized inguinal lymph node (LN) flap was transferred into the ipsilateral fossa after a popliteal LN was removed; a LN dissection (LND) model in which the popliteal LN was dissected; and a control model in which a skin incision was made at the popliteal fossa and an ipsilateral inguinal LN was removed. Postoperative lymphatic flows were observed by indocyanine green lymphography and B16-F10-luc2 mouse melanoma were implanted into the ipsilateral footpad. The proportion of DCs in the transplanted nodes was measured by CD11c immunohistochemistry using digital imaging analysis 4 days after cancer implantation. Metastases to the lungs and LNs were quantitatively evaluated by luciferase assay 4 weeks after cancer implantation.

***Results:*** After VLNT, lymphatic reconnection was observed in 59.2% of mice. The proportion of DCs was significantly higher in the VLNT group with lymphatic reconnection (8.6% ± 1.0%) than in the naïve LN (4.3% ± 0.4%) ($P < 0.001$). The tumor burden of lung metastases was significantly less in the VLNT group with lymphatic reconnection compared with the LND group ($P = 0.049$).

***Conclusions:*** Metastasis decreased in mice with reconnected lymphatics after VLNT. A possible explanation was that lymphatic restoration may have contributed to the tumor immune response by allowing DC migration to LNs.

***Keywords:*** lymphatic system, lymph nodes, melanoma, mice, vascularized composite allotransplantation

## Introduction

Lymph flows through a network of afferent lymphatic vessels, lymph nodes (LNs), and efferent lymphatic vessels, before entering the thoracic duct, from which it drains directly into the venous system. This network is also involved in immune surveillance, importing various antigens and activated antigen-presenting cells into the LNs and exporting immune effector cells and factors involved in the humoral response into the blood circulation.[1-5] Therefore, impairment of the regional lymphatic system causes not only swelling of the extremities but also impaired immune surveillance, which leads to various immune disorders, chronic inflammatory conditions, and neoplasms.[1,6-8] A study of immune cells in the peripheral LNs and skin of 17 patients with lymphedema suggested impaired lymphocyte and Langerhans cell trafficking, presumably resulting in ineffective removal of foreign antigens.[6] Clinically, secondary lymphedema has been reported to predispose to the development of malignant tumors such as Kaposi's sarcoma, malignant melanoma, Merkel cell carcinoma, and malignant lymphoma.[8-11] Animal experiments in several studies have shown that lymphatic impairment carries a risk of tumor dissemination and metastasis.[12-15] In a mouse model with melanoma implanted into the footpad, the amount of lung metastasis was significantly greater at 24 days in the lymphedema model than in the non-lymphedema model.[14]

Modern microsurgical lymphatic reconstruction procedures can achieve marked improvement in lymphedema.[4,16,17] Vascularized LN transfer (VLNT) is indicated in patients with moderate to advanced lymphedema that is unlikely to respond to other treatments.[18-21] VLNT is thought to facilitate the spontaneous regeneration of lymphatic vessels from existing capillary lymph vessels and lymphatic endothelial progenitor cells, promoting physiologic recovery by restoring the regional lymphatic network.[22] Within a cohort of lymphedema patients ($n$ = 42), the infection rate was effectively suppressed from 74% to 5% after VLNT.[23] Although some

experimental studies support the immunological impact of VLNT, no study has investigated whether VLNT itself has an impact on anti-cancer immunity.

In the present study, we first observed cancer dynamics after VLNT in mouse models, focusing on the restoration of regional lymphatics. We created a VLNT model in C57BL/6N mice using established and reproducible methods for the evaluation of lymphatic reconnection.[25] This mouse model can be used to create a tumor transplantation model using B16-F10 murine melanoma cells, which metastasize preferentially to the lungs and LNs. We therefore thought that this model would be useful for studying anti-cancer immunity, which is difficult to investigate in clinical studies.

Among immune cells, dendritic cells (DCs) play an important role in the early tumor immune response. Peripherally activated DCs that recognize tumor antigens migrate through afferent lymphatic vessels into the LNs, where they present antigens and activate lymphocytes.[26-28] It has been found in a mouse model that reduced migration of DCs to LNs leads to impairment of T cell responses and suppresses adaptive immune responses.[29] We focused on DC dynamics against cancer to verify whether an early tumor immune response is at work after VLNT. We also examined lung and LN metastases to evaluate systemic anti-cancer immunity. We hypothesized that local immune surveillance was at work in mice after VLNT compared with mice in which the regional lymphatics had been dissected.

## Materials and Methods

All experiments were approved by the Institutional Animal Care and Use Committee at Hokkaido University and conducted in accordance with the Guidelines for the Care and Use of Laboratory Animals. Male C57BL/6N mice (age 6 weeks, weight 20–22 g, $n = 51$) were purchased from Sankyo Labo Service (Tokyo, Japan) and used after a 2-week acclimation period. Mice were maintained in specific pathogen-free conditions with an artificial 12-h

light/dark cycle. All experiments were performed under general anesthesia by inhalation of 2%–3% (flow rate) isoflurane.

***Experimental design and surgical procedures***

The experimental design is shown in Figure 1. Mice were allocated to a control group ($n$ = 12), a VLNT group ($n$ = 27), an LND group ($n$ = 8), and a sham surgery group ($n$ = 4). In the control group, a skin incision was made at the left popliteal fossa and a left inguinal LN was removed to match the conditions of the other groups (Figure 2A). In the VLNT group, the surgical procedure performed has been described in detail previously.[25] Briefly, an inguinal LN-bearing flap with a vascular pedicle containing the superficial caudal epigastric vessels was transferred into the left popliteal fossa after excision of a popliteal LN (Figure 2B and Figure 3). In the LND group, a left popliteal LN was resected with the surrounding fat pad and a left inguinal LN was also removed (Figure 2C)

***Indocyanine green lymphography and final grouping of the models***

Three weeks postoperatively, we assessed the flow of lymph in the hind limbs of each mouse using indocyanine green (ICG) lymphography as previously reported.[25] Fluorescence images were obtained using a near-infrared fluorescence camera system after subcutaneous injection of 5 μL of ICG solution (Daiichi Sankyo Co., Ltd., Tokyo, Japan; 2.5 mg/mL in distilled water) into both hind paws in each mouse. In the VLNT group, afferent lymphatic reconnection was confirmed if a clear spot could be seen in the popliteal fossa. The mice in the VLNT group were then categorized as lymphatic reconnection-positive (VLNT(lr+)) or lymphatic reconnection-negative (VLNT(lr−)).

***Preparation of murine melanoma cells***

The B16-F10-luc2 (murine melanoma) cell line was purchased from Caliper Lifesciences (Hopkinton, MA) and the B16-F10 cell line was obtained from the American Type Culture Collection (ATCC, Rockville, MD). B16-F10-luc2 murine melanoma was generated by transducing a lentivirus containing the luc2 gene under control of the human ubiquitin C promoter. The cell line was maintained in RPMI 1640 medium (ATCC, Rockville, MD) containing 5% fetal bovine serum and 1% penicillin/streptomycin at 37°C under 5% $CO_2$. Four weeks postoperatively, a suspension containing the melanoma cells was injected into the left hindlimb footpad at a dose of $4 \times 10^5$ cells in 0.05 mL of phosphate-buffered saline. In a previous study, lung metastases were predominantly exacerbated in LND mice compared to normal mice at 4 weeks after implantation of melanoma cells in the footpad, so we used the same dose of the cells in the present study.[14]

***Immunohistochemical analysis of transplanted LNs***

The mice ($n$ = 15) were euthanized 4 days after implantation of the melanoma cells for immunohistochemical analysis. A popliteal LN (in the control group) or a transplanted LN (in the (VLNT(lr+) and VLNT(lr−) subgroups) was collected from each mouse. Popliteal LNs from non-tumor-bearing sham surgery mice ($n$ = 4) were designated as naïve popliteal LNs and were collected 4 days after saline injection into the hindlimb footpad.

The specimens were fixed with 4% paraformaldehyde, embedded in paraffin, and cut into 4-μm sections. The sections were then stained using immunohistochemical dyes for DCs with CD11c (hamster monoclonal CD11c antibody [clone N418, code GTX74940, 1:300, GeneTex Inc., Irvine, CA]) overnight at 4°C. The histology slides were scanned and digital images were analyzed using NDP.view2 software. After TIFF images were captured, the percentages of DCs in each LN specimen were quantified using ImageJ software (version 1.52; National Institutes of Health, Bethesda, MD) as described previously.[30]

### *Quantification of metastases to the LNs and lung*

Four weeks after injection of melanoma cells, the mice ($n$ = 32) were euthanized for *ex vivo* luciferase assay. An LN in the left popliteal fossa, a left lumbar LN, a left axillary LN and a lung were collected. Each harvested specimen was washed in phosphate-buffered saline and frozen immediately using liquid nitrogen. The specimens were crushed using a Micro Smash MS-100 system (Tomy, Tokyo, Japan) and then lysed in Luciferase Cell Culture Lysis Reagent (E1500, Promega, Madison, WI; 800 μL for the lung specimens, 200 μL for LNs) and vortexed for 15 min. The centrifuged supernatant was transferred and luciferase activity was calculated as relative light units (RLU) using a GloMax20/20 Luminometer (Promega, Madison, WI) using a previously reported technique.[31]

### *Statistical analysis*

All quantitative data are presented as the mean ± standard deviation (SD). All quantitative measurements *in vitro* were performed by two examiners blindly. For evaluation of metastasis, the data were subjected to natural logarithm transformation prior to statistical processing because the tumor exhibited exponential growth.[32] Dunnett's test was used for analysis of lung metastasis and immunohistochemical data. The Steel–Dwass test was used to examine metastasis to the LNs because of wide interindividual variation. All statistical analyses were performed using JMP® Pro 14.0.0 software (SAS Institute Inc., Cary, NC). A $P$-value < 0.05 (two-tailed) was considered statistically significant.

## Results

### *Regional lymphatics was restored in 59.2% of mice after VLNT*

In the control group, ICG lymphography revealed clear spotted fluorescence in the intact

popliteal region, and no lymphatic abnormality caused by removal of an inguinal LN was observed. In the VLNT group, 16 mice (59.2%) showed a clear spot similar to that in the area of the intact popliteal LN; all these mice were deemed to be the VLNT(lr+) subgroup. A collateral lymphatic vessel was observed in 1 VLNT(lr+) mouse. The remaining 11 mice (40.7%) in the VLNT group did not show a clear spot, had a dermal backflow pattern, and/or collateral vessels in the lower extremity that were not connected to the popliteal LN; these mice were deemed to be the VLNT(lr−) subgroup. In the LND group, a dermal backflow pattern and collateral vessels similar to those in the VLNT(lr−) subgroup were observed (Figure 4).

***DCs were significantly elevated in transplanted LNs in VLNT(lr+) mice in the premetastatic phase***

Immunohistochemical staining of the LNs for CD11c showed numerous positive-staining cells in the paracortex and subcapsular sinus of the popliteal LN in the control group and of the transplanted node in the VLNT(lr+) subgroup. In contrast, few positive-staining cells were detected in the transplanted node in the VLNT(lr−) subgroup. (Figure 5). Without cancer sensitization, the proportion of DCs in the naïve popliteal LN was 4.3% ± 0.4%; with cancer sensitization, the proportion in the node was 8.7% ± 0.6% in the control group, 8.6% ± 1.0% in the VLNT(lr+) subgroup, and 3.5% ± 0.9% in the VLNT(lr−) subgroup. With cancer sensitization, the percentage of DCs was significantly higher in the control group ($P < 0.001$) and the VLNT(lr+) subgroup ($P < 0.001$) than in naïve popliteal LNs without cancer sensitization. There was no significant change in the node of the VLNT(lr-) subgroup ($P = 0.40$) (Figure 6).

***Mice with restored lymph flow after VLNT had fewer distant metastases***

The tumor burden in the popliteal LNs was 665 ± 1,101 RLU in the control group, 390 ± 525 RLU in the VLNT(lr+) subgroup, and 101 ± 6 RLU in the VLNT(lr−) subgroup. (Figure 6A). The tumor burden in the axillary LN was 96 ± 8 RLU in the control group, 178 ± 234 RLU in the VLNT(lr+) subgroup, 614,916 ± 1,504,625 RLU in the VLNT(lr−) subgroup, and 786,742 ± 2,032,902 RLU in the LND group, indicating a significantly higher metastasis burden in the VLNT(lr−) subgroup and the LND group ($P = 0.041$ and $P = 0.011$, respectively; Figure 6B). The tumor burden in the lumbar LN was 139 ± 80 RLU in the control group, 200 ± 290 RLU in the VLNT(lr+) subgroup, 1,338 ± 2,031 RLU in the VLNT(lr−) subgroup, and 419 ± 371 RLU in the LND group. (Figure 6C). The tumor burden in the lung was 1,607 ± 2,926 RLU in the control group, 1,463 ± 1,985 RLU in the VLNT(lr+) subgroup, 1,328,595 ± 3,248,491 RLU in the VLNT(lr−) subgroup, and 2,255,699 ± 3,862,454 RLU in the LND group. The quantitative value of the lung metastasis burden was significantly lower in the control group and VLNT(lr+) subgroup than in the LND group ($P = 0.047$ and $P = 0.049$, respectively; Figure 7).

## Discussion

In this study, we found that by inducing reconnection of lymphatic vessels after VLNT, the regional lymphatic network was restored and DCs increased in the transplanted nodes after cancer implantation. In addition, there was significantly less distant lung metastases compared with the LN dissection models.

ICG lymphography performed 3 weeks after surgical intervention revealed that mice in the VLNT(lr−) subgroup, in whom lymphatic vessel regeneration did not occur, showed a similar lymphatic flow pattern to that in the LND group; both showed a dermal backflow pattern, which indicates regional lymph stasis, and rerouting of lymphangiogenesis, which is not observed in the intact lymphatic network. These findings are consistent with previous reports

of regional lymphatic disruption after surgical intervention.[25,33,34] However, in the VLNT(lr+) subgroup, the transplanted LN was observed to be similar to an intact popliteal LN; although one mouse showed rerouting of lymphangiogenesis, there were no cases of lymph stasis, indicating that normal lymphatic flow was successfully restored in this group. Clinically, one of the main reasons why VLNT is useful is that the transplanted LNs serve as a scaffold that promotes the regeneration of lymphatic vessels from existing capillary lymph vessels and lymphatic endothelial progenitor cells, thereby contributing to reconstruction of the local lymphatic network.[35,36] In the VLNT(lr+) subgroup, VLNT successfully reconstructed an intact lymphatic system consisting of lymphatic vessels and LNs. Ishikawa *et al.* reported that the success rate of lymphatic reconnection in the same model ($n$ = 25) was 64%, which is roughly equal to the rate in our study.[25]

It is known that lymphatic vessels, especially afferent lymphatic vessels, contribute to peripheral tissue immunity by providing a local anatomical framework for immune surveillance and adaptive immune response. DCs that recognize antigens in peripheral tissues migrate through afferent lymph vessels to the paracortical area of LNs and rapidly activate adaptive immune responses upon arrival.[37] Here, the normal functioning of lymphatic vessels not only serves as a passive route for immune cells and lymph but also actively impacts antigen distribution and presentation, the direct modulation of DC trafficking and activation, and leukocyte interactions.[38-40] In our experiment, after cancer implantation, the percentage of DCs in transplanted LNs of VLNT(lr+) subgroup was significantly higher, as in the control group with an intact popliteal node. In addition, DCs were observed to be distributed in the paracortical area. In contrast, there was no obvious distribution nor an increase of DCs in the VLNT(lr−) subgroup. Among immune cells, DCs play an important role in the early tumor immune response. The normal lymphatic anatomy that is restored by the VLNT may contribute via these immune cells for early immunological recognition and the mounting of a

robust immune response.

Metastases were found in the transplanted LN and the popliteal LN in the control group, whereas in the VLNT(lr−) subgroup, there were almost no metastases in the transplanted LN, although metastases to superior LNs such as the lumbar LNs were increased. These results indicate that the transplanted LN successfully served as a substitute for the sentinel LN by receiving the first lymphatic inflow.[31,41] Changes in lymphatic flow pathways can also be confirmed by changes in the pathways of LN metastases. Our ICG findings showed the development of lymphangiogenic rerouting at the site of lymphatic disruption, and the amount of metastasis to the axillary LN was significantly greater in the VLNT(lr−) subgroup and the LND group compared with the control group. In these groups, the regional lymphatic system may have failed to repair itself after being damaged by surgical intervention, and this caused the formation of an abnormal lymphatic network to the axillary LN. In fact, given that the lymphatic channel is a pathway for metastasis, lymphadenectomy has been shown to alter the metastatic pathway and increase distant LN metastasis from the original route.[4,31,34] Taken together, our results suggest that in the VLNT(lr−) subgroups and the LND group, the lymphatic network was not properly reconstituted and thus systemic metastasis was exacerbated by inadequate functioning of the local immune system. In the future, VLNT may be recommended for lymphedema patients with high-grade primary melanoma and high risk of recurrence from the perspective of tumor control.

This study has several limitations. First, LNs are smaller in mice than in humans and the experimental system used was simpler than the human lymphatic system, so interpretation of the results is limited to the scope of animal experiments. Second, we observed cancer dynamics in the mouse models from the viewpoint of restoring regional lymphatics and the percentage change in DCs in proximal LNs. A more detailed evaluation of the immune cells involved in the anti-cancer effect will be included in a future study so that we can discuss

anti-cancer immunity. Third, in the present study we did not use a lymphedema model because of the complexity of the procedure and the significant deviation from the VLNT model used in this study.[42] In an actual lymphedematous state, the mechanism of carcinogenesis is complex and does not depend on a single trigger. Finally, metastasis was evaluated at only the 4-week time point after cancer transplantation, so other evaluation time points may need to be considered.

## Conclusion

We found that metastasis was decreased in mice with succeeded lymphatic reconnection after VLNT. A possible explanation for this was that restoration of the lymphatic system may have contributed to the tumor immune response by allowing DC migration to sentinel LNs. This a preliminary finding in a small study in mouse models and needs further validation.

## References


1. Azhar SH, Lim HY, Tan BK, Angeli V. The unresolved pathophysiology of lymphedema. Front Physiol 2020;11:137.
2. Witte MH, Bernas MJ, Martin CP, Witte CL. Lymphangiogenesis and lymphangiodysplasia: from molecular to clinical lymphology. Microsc Res Tech 2001;55:122–145.
3. Oliver G, Detmar M. The rediscovery of the lymphatic system: old and new insights into the development and biological function of the lymphatic vasculature. Genes Dev 2002;16:773–783.
4. Alitalo K. The lymphatic vasculature in disease. Nat Med 2011;17:1371–1380.
5. Tammela T, Alitalo K. Lymphangiogenesis: molecular mechanisms and future promise. Cell 2010;140:460–476.
6. Olszewski WL, Engeset A, Romaniuk A, Grzelak I, Ziolkowska A. Immune cells in peripheral lymph and skin of patients with obstructive lymphedema. Lymphology 1990;23:23–33.
7. Ruocco E, Puca RV, Brunetti G, Schwartz RA, Ruocco V. Lymphedematous areas: privileged sites for tumors, infections, and immune disorders. Int J Dermatol 2007;46:662.
8. Ruocco V, Schwartz RA, Ruocco E. Lymphedema: an immunologically vulnerable site for development of neoplasms. J Am Acad Dermatol 2002;47:124–127.
9. Saito Y, Nakagami H, Kaneda Y, Morishita R. Lymphedema and therapeutic lymphangiogenesis. Biomed Res Int 2013;2013:804675.
10. Stewart FW, Treves N. Lymphangiosarcoma in postmastectomy lymphedema; a report of six cases in elephantiasis chirurgica. Cancer 1948;1:64–81.
11. Schiffman S, Berger A. Stewart-Treves syndrome. J Am Coll Surg 2007;204:328.

12. Rofstad EK, Tunheim SH, Mathiesen B, Graff BA, Halsør EF, Nilsen K, Galappathi K. Pulmonary and lymph node metastasis is associated with primary tumor interstitial fluid pressure in human melanoma xenografts. Cancer Res 2002;62:661–664.
13. Zhu Y, Zhao T, Itasaka S, Zeng L, Yeom CJ, Hirota K, Suzuki K, Morinibu A, Shinomiya K, Ou G, Yoshimura M, Hiraoka M, Harada H. Involvement of decreased hypoxia-inducible factor 1 activity and resultant G1-S cell cycle transition in radioresistance of perinecrotic tumor cells. Oncogene 2013;32:2058–2068.
14. Oashi K, Furukawa H, Nishihara H, Ozaki M, Oyama A, Funayama E, Hayashi T, Kuge Y, Yamamoto Y. Pathophysiological characteristics of melanoma in-transit metastasis in a lymphedema mouse model. J Invest Dermatol 2013;133:537–544.
15. Kimura T, Sugaya M, Oka T, Blauvelt A, Okochi H, Sato S. Lymphatic dysfunction attenuates tumor immunity through impaired antigen presentation. Oncotarget 2015;6:18081–18093.
16. Di Taranto G, Bolletta A, Chen SH, Losco L, Elia R, Cigna E, Rubino C, Ribuffo D, Chen HC. A prospective study on combined lymphedema surgery: gastroepiploic vascularized lymph nodes transfer and lymphaticovenous anastomosis followed by suction lipectomy. Microsurgery 2021;41:34–43.
17. Ciudad P, Manrique OJ, Bustos SS, Coca JJP, Chang CC, Shih PK, Nicoli F, Torto FL, Agko M, Huang TCT, Maruccia M, Chen HC. Comparisons in long-term clinical outcomes among patients with upper or lower extremity lymphedema treated with diverse vascularized lymph node transfer. Microsurgery 2020;40:130–136.
18. Becker C. Microlymphatic surgery for the treatment of iatrogenic lymphedema. Clin Plastic Surg 2012;39:385–398.
19. Akita S, Yamaji Y, Tokumoto H, Sasahara Y, Kubota Y, Kuriyama M, Mitsukawa N. Improvement of the efficacy of vascularized lymph node transfer for lower-extremity

lymphedema via a prefabricated lympho-venous shunt through lymphaticovenular anastomosis between the efferent lymphatic vessel and small vein in the elevated vascularized lymph node. Microsurgery 2018;38:270–277.

20. Scaglioni MF, Arvanitakis M, Chen YC, Giovanoli P, Chia-Shen Yang J, Chang EI. Comprehensive review of vascularized lymph node transfers for lymphedema: Outcomes and complications. Microsurgery 2018;38:222–229.

21. Li Y, Dong R, Li Z, Wang L, Long X. Intra-abdominal vascularized lymph node transfer for treatment of lymphedema: a systematic literature review and meta-analysis. Microsurgery 2021;41:802–815.

22. Aschen SZ, Farias-Eisner G, Cuzzone DA, Albano NJ, Ghanta S, Weitman ES, Ortega S, Mehrara BJ. Lymph node transplantation results in spontaneous lymphatic reconnection and restoration of lymphatic flow. Plast Reconstr Surg 2014;133:301–310.

23. Nguyen AT, Suami H, Hanasono MM, Womack VA, Wong FC, Chang EI. Long-term outcomes of the minimally invasive free vascularized omental lymphatic flap for the treatment of lymphedema. J Surg Oncol 2017;115:84–89.

24. Hayashida K, Yoshida S, Yoshimoto H, Fujioka M, Saijo H, Migita K, Kumaya M, Akita S. Adipose-derived stem cells and vascularized lymph node transfers successfully treat mouse hindlimb secondary lymphedema by early reconnection of the lymphatic system and lymphangiogenesis. Plast Reconstr Surg 2017;139:639–651.

25. Ishikawa K, Maeda T, Funayama E, Hayashi T, Murao N, Osawa M, Furukawa H, Oyama A, Yamamoto Y. Feasibility of pedicled vascularized inguinal lymph node transfer in a mouse model: a preliminary study. Microsurgery 2019;39:247–254.

26. Lund AW, Wagner M, Fankhauser M, Steinskog ES, Broggi MA, Spranger S, Gajewski TF, Alitalo K, Eikesdal HP, Wiig H, Swartz MA. Lymphatic vessels regulate immune microenvironments in human and murine melanoma. J Clin Invest 2016;126:3389–

3402.

27. Cochran AJ, Huang RR, Lee J, Itakura E, Leong SP, Essner R. Tumour-induced immune modulation of sentinel lymph nodes. Nat Rev Immunol 2006;6:659–670.

28. Randolph GJ, Angeli V, Swartz MA. Dendritic-cell trafficking to lymph nodes through lymphatic vessels. Nat Rev Immunol 2005;5:617–628.

29. Teoh D, Johnson LA, Hanke T, McMichael AJ, Jackson DG. Blocking development of a CD8+ T cell response by targeting lymphatic recruitment of APC. J Immunol 2009;182:2425–2431.

30. Ishikawa K, Funayama E, Maeda T, Hayashi T, Murao N, Osawa M, Ito R, Furukawa H, Oyama A, Yamamoto Y. Changes in high endothelial venules in lymph nodes after vascularized and nonvascularized lymph node transfer in a murine autograft model. J Surg Oncol 2019;119:700–707.

31. Maeda T, Hayashi T, Furukawa H, Iwasaki D, Ishikawa K, Funayama E, Murao N, Osawa M, Oyama A, Yamamoto Y. Immune-mediated antitumor effect of a transplanted lymph node. Int J Cancer 2018;143:1224–1235.

32. Feng C, Wang H, Lu N, Chen T, He H, Lu Y, Tu XM. Log-transformation and its implications for data analysis. Shanghai Arch Psychiatry 2014;26:105–109.

33. Blum KS, Proulx ST, Luciani P, Leroux JC, Detmar M. Dynamics of lymphatic regeneration and flow patterns after lymph node dissection. Breast Cancer Res Treat 2013;139:81–86.

34. Kwon S, Agollah GD, Wu G, Sevick-Muraca EM. Spatio-temporal changes of lymphatic contractility and drainage patterns following lymphadenectomy in mice. PloS One 2014;9:e106034.

35. Ito R, Suami H. Overview of lymph node transfer for lymphedema treatment. Plast Reconstr Surg 2014;134:548–556.

36. Miranda Garces M, Pons G, Mirapeix R, Masia J. Intratissue lymphovenous communications in the mechanism of action of vascularized lymph node transfer. J Surg Oncol 2017;115:27–31.
37. Steele MM, Lund AW. Afferent lymphatic transport and peripheral tissue immunity. J Immunol 2021;206:264–272.
38. Podgrabinska S, Kamalu O, Mayer L, Shimaoka M, Snoeck H, Randolph GJ, Skobe M. Inflamed lymphatic endothelium suppresses dendritic cell maturation and function via Mac-1/ICAM-1-dependent mechanism. J Immunol 2009;183:1767–1779.
39. Miteva DO, Rutkowski JM, Dixon JB, Kilarski W, Shields JD, Swartz MA. Transmural flow modulates cell and fluid transport functions of lymphatic endothelium. Circ Res 2010;106:920–931.
40. O'Melia MJ, Lund AW, Thomas SN. The biophysics of lymphatic transport: engineering tools and immunological consequences. iScience 2019;22:28–43.
41. Harrell MI, Iritani BM, Ruddell A. Tumor-induced sentinel lymph node lymphangiogenesis and increased lymph flow precede melanoma metastasis. Am J Pathol 2007;170:774–786.
42. Oashi K, Furukawa H, Oyama A, Funayama E, Hayashi T, Saito A, Yamamoto Y. A new model of acquired lymphedema in the mouse hind limb: a preliminary report. Ann Plast Surg 2012;69:565–568.

**Figure Legends**

**Figure 1.** Schematic of the study design. Groupings in Experiment 1 and Experiment 2, n, and time points for evaluation. DCs, dendritic cells. Exp, Experiment. ICG, indocyanine green. LN, lymph node. LND, lymph node dissection. VLNT, vascularized lymph node transfer. VLNT(lr+), vascularized lymph node transfer with lymphatic reconnection subgroup. VLNT(lr-), vascularized lymph node transfer without lymphatic reconnection subgroup.

**Figure 2.** Schematic of the surgical techniques. *A,* Control group. *B,* Vascularized lymph node transfer group. *C,* Lymph node dissection group. ILN, inguinal lymph node. PLN, popliteal lymph node.

**Figure 3.** Intraoperative photo of vascularized lymph node transfer. *A*, An inguinal lymph node-bearing flap with a vascular pedicle containing the superficial caudal epigastric vessels (arrows) was elevated. *B*, The lymph node-bearing flap was then transferred into the popliteal fossa (arrowhead). ILN, inguinal lymph node.

**Figure 4.** Indocyanine green lymphography images of the hindlimbs in the prone position in each group 3 weeks postoperatively. *A*, control group. *B*, lymph node dissection group. *C*, vascularized lymph node transfer with lymphatic reconnection subgroup. *D*, vascularized lymph node transfer without lymphatic reconnection subgroup. Arrowheads show the transplanted lymph node appearing as a clear spot, which indicates successful afferent lymphatic reconnection. Arrows indicate the collateral vessels of lymphatic rerouting where the dermal backflow pattern was observed.

**Figure 5.** Immunohistochemical staining of lymph nodes from the popliteal fossa for dendritic cells (CD11c). Bars, 500 μm. *A*, naïve lymph node (no melanoma implantation). *B*, control group. *C*, vascularized lymph node transfer with lymphatic reconnection subgroup. *D*, vascularized lymph node transfer without lymphatic reconnection subgroup.

**Figure 6.** Percentages of dendritic cells in lymph nodes in the popliteal fossa detected by immunohistochemical analysis. Data are presented as box-and-whisker plots. Boxes represent interquartile ranges (25th to 75th percentiles). A horizontal line across a box indicates the median, and the whiskers extend from the box to the highest and lowest nonoutlier values. $n = 4–7$, $*P < 0.0001$, $**P < 0.0001$ (Dunnett's test). LN, lymph node; VLNT(lr+), vascularized lymph node transfer with lymphatic reconnection; VLNT(lr−), vascularized lymph node transfer without lymphatic reconnection.

**Figure 7.** Metastasis to lymph nodes in the popliteal fossa (*A*), axillary lymph nodes (*B*), and lumbar lymph nodes (*C*). Total luciferase activity was determined with standard *ex vivo* luciferase assay. Data are presented as box-and-whisker plots. Boxes represent interquartile ranges (25th to 75th percentiles). A horizontal line across a box shows the median, and whiskers extend from the box to the highest and lowest nonoutlier values. Outliers are shown as a circle. $n = 7–9$, $*P = 0.041$, $**P = 0.011$, $***P = 0.04$ (Steel–Dwass test). LNs, lymph nodes. LND, lymph node dissection; RLU, relative light units; VLNT(lr+), vascularized lymph node transfer with lymphatic reconnection; VLNT(lr−), vascularized lymph node transfer without lymphatic reconnection.

**Figure 8.** Analysis of lung metastasis by luciferase assay. Total luciferase activity was determined by standard ex vivo luciferase assay. The graphs show the mean ± standard error

of the mean values for natural logarithmic converted data. $n$ = 7–9, *$P$ = 0.047, **$P$ = 0.049 (Dunnett's test). LND, lymph node dissection; RLU, relative light units; VLNT(lr+), vascularized lymph node transfer with lymphatic reconnection; VLNT(lr−), vascularized lymph node transfer without lymphatic reconnection.

## Exp. 1: Histological analysis of LN (n = 19)

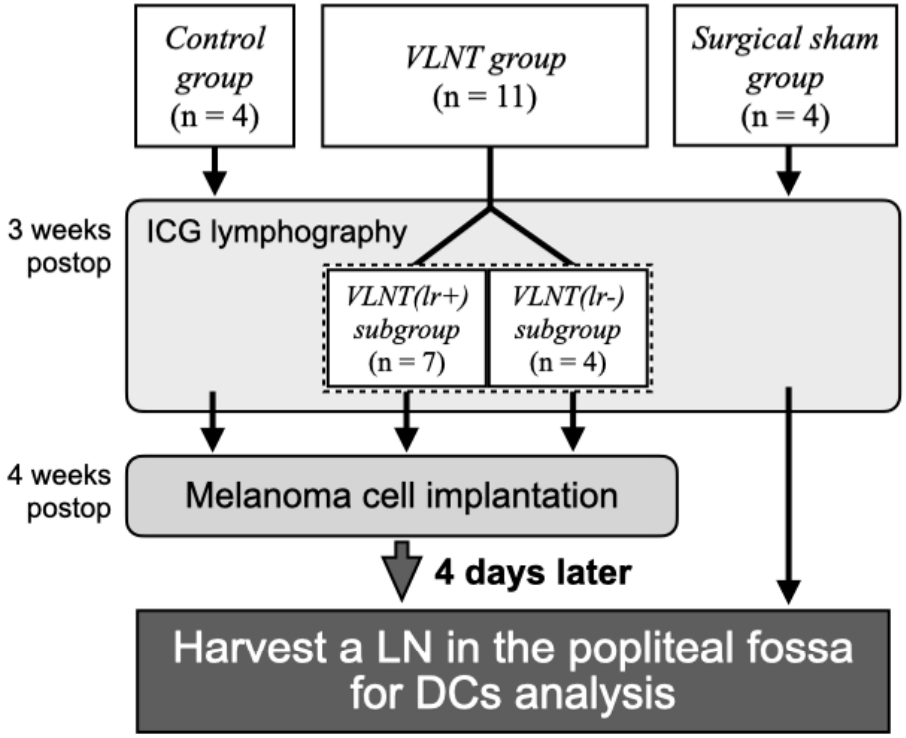


## Exp. 2: Quantification of metastasis (n = 32)

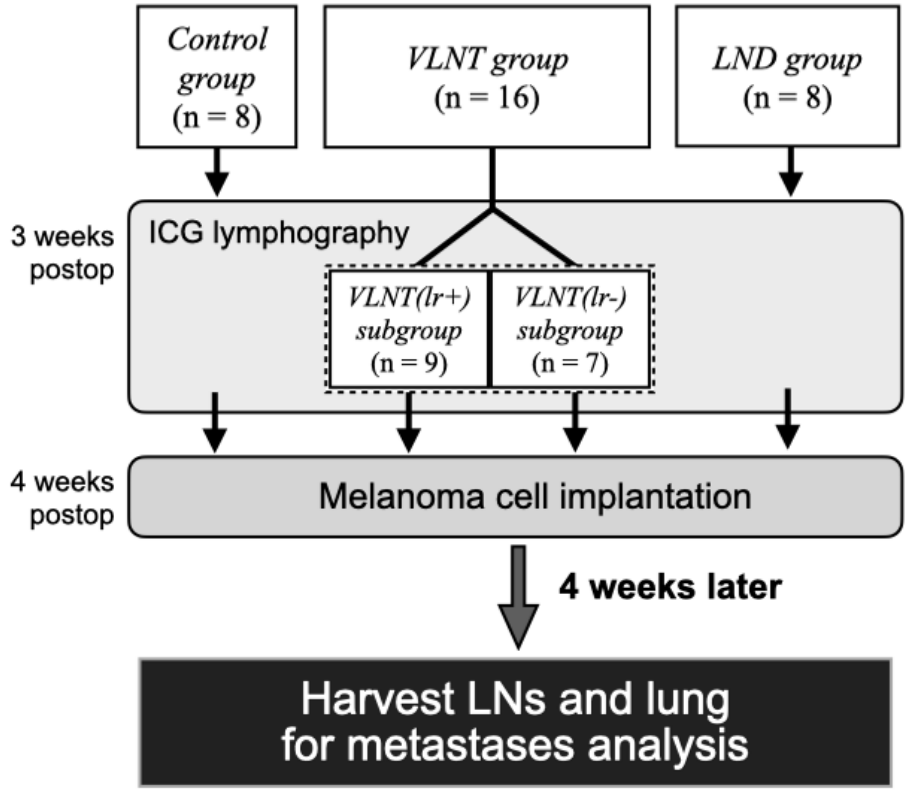

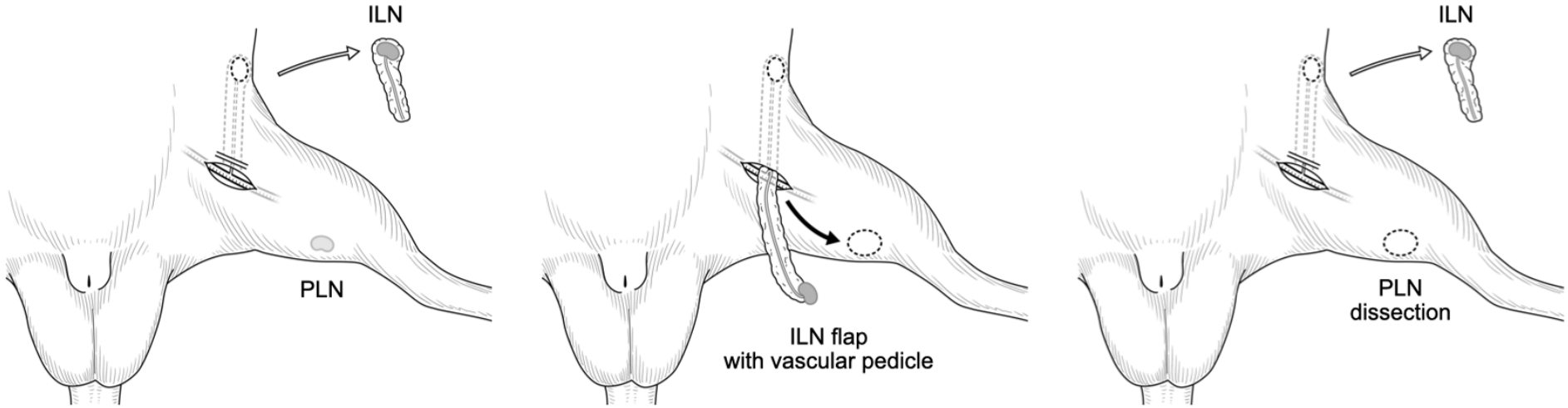


*A. Control group*

*B. VLNT group*

*C. LND group*

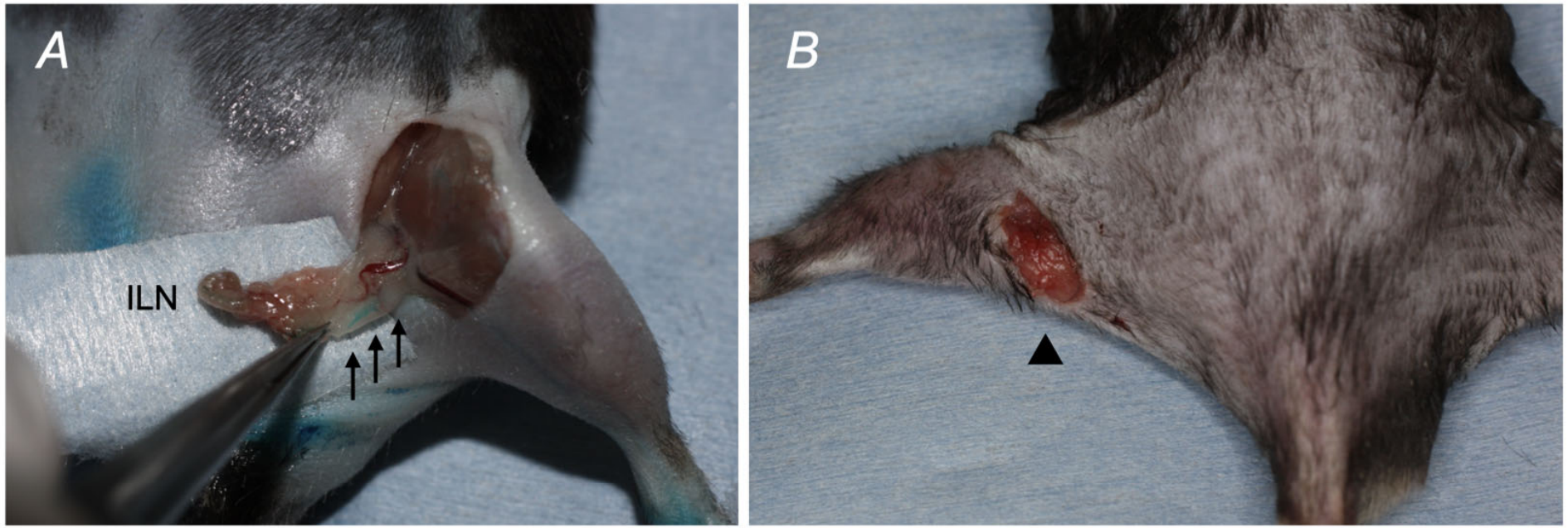
A
ILN
B

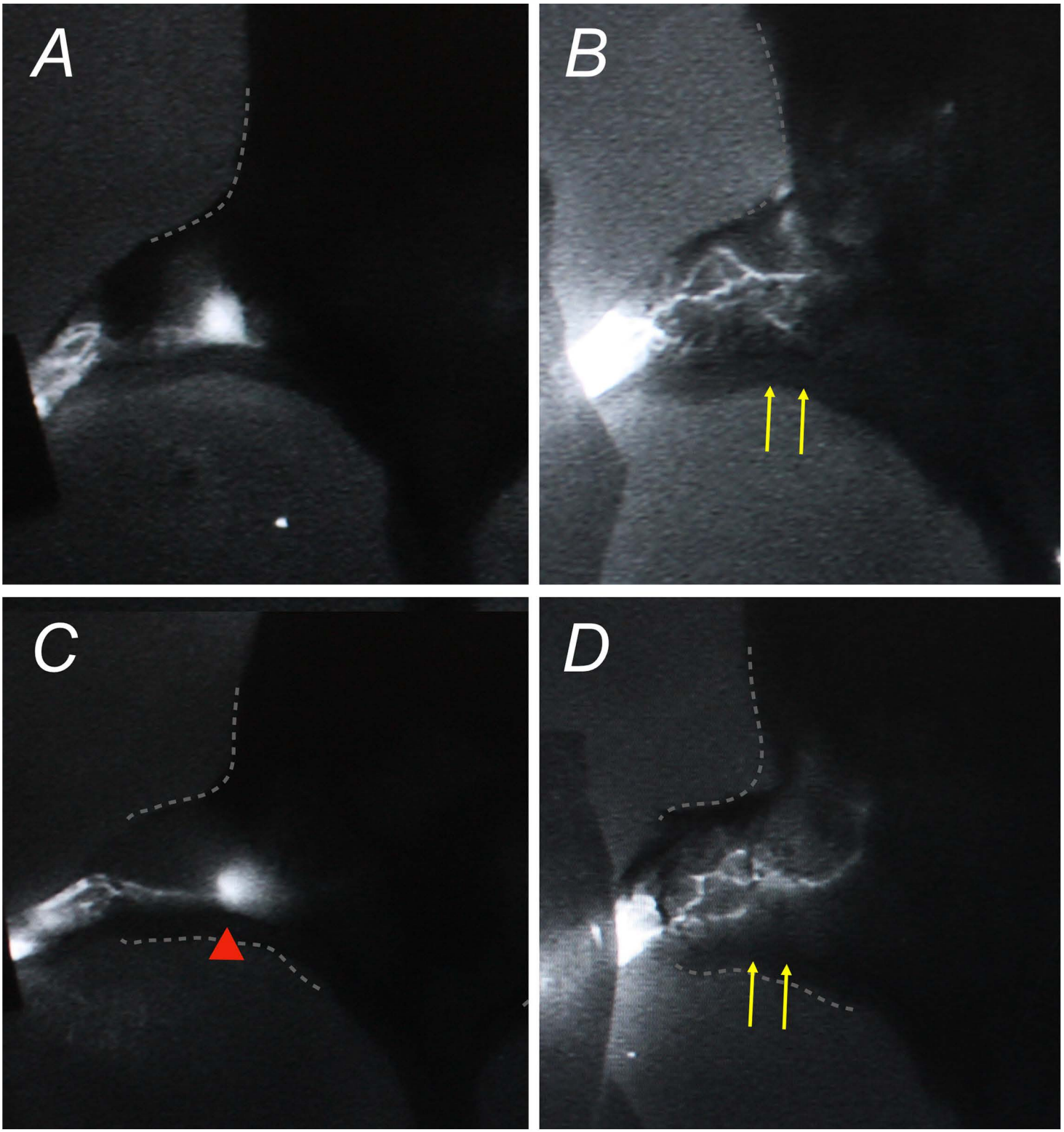
A
B
C
D

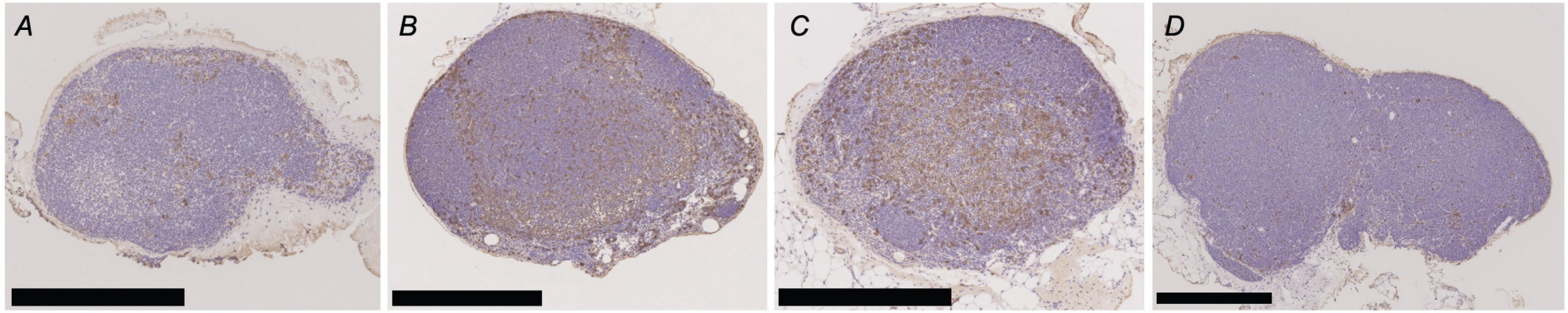
A
B
C
D

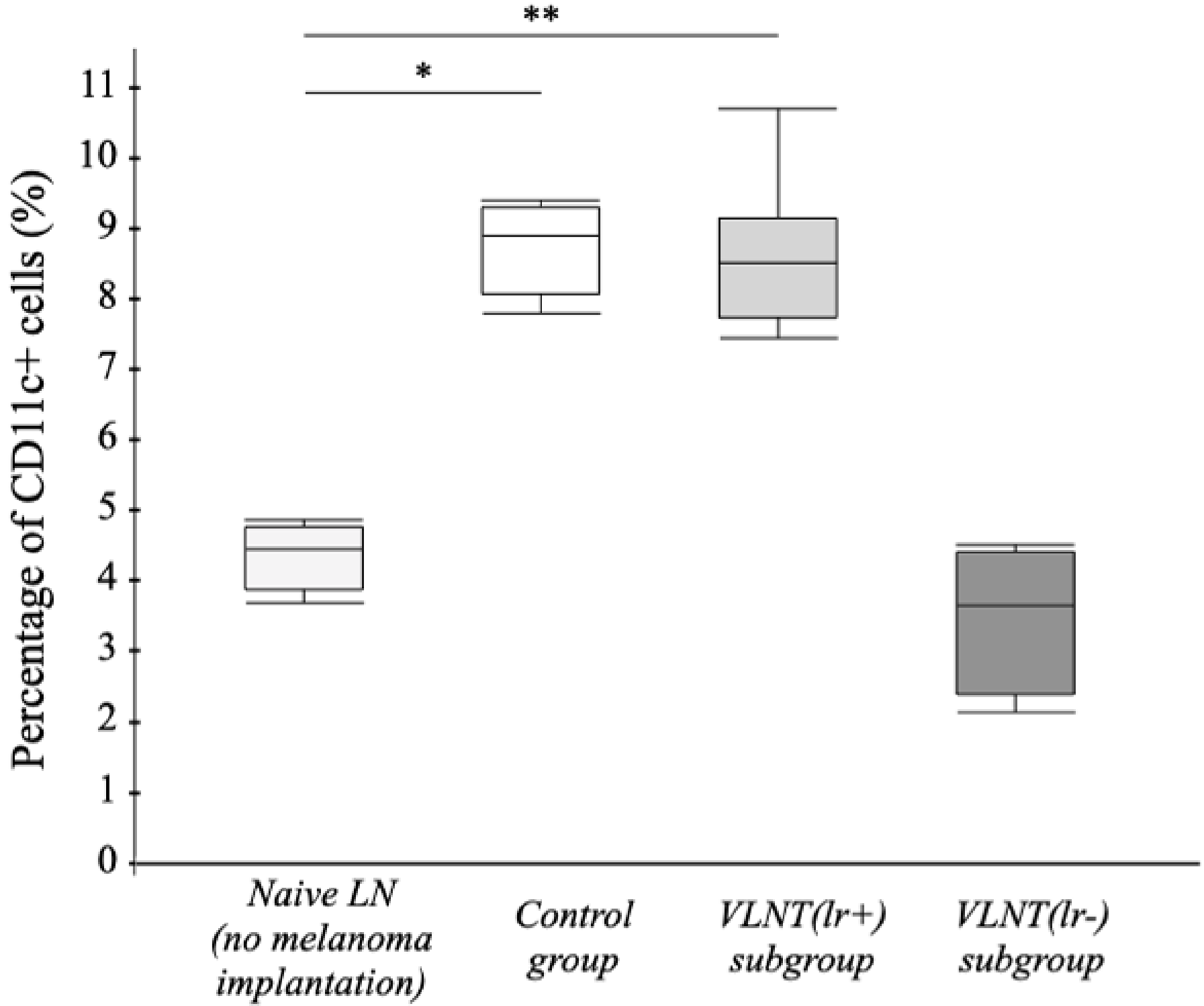
**
*
Percentage of CD11c+ cells (%)
11
10
9
8
7
6
5
4
3
2
1
0
Naive LN (no melanoma implantation)
Control group
VLNT(lr+) subgroup
VLNT(lr-) subgroup

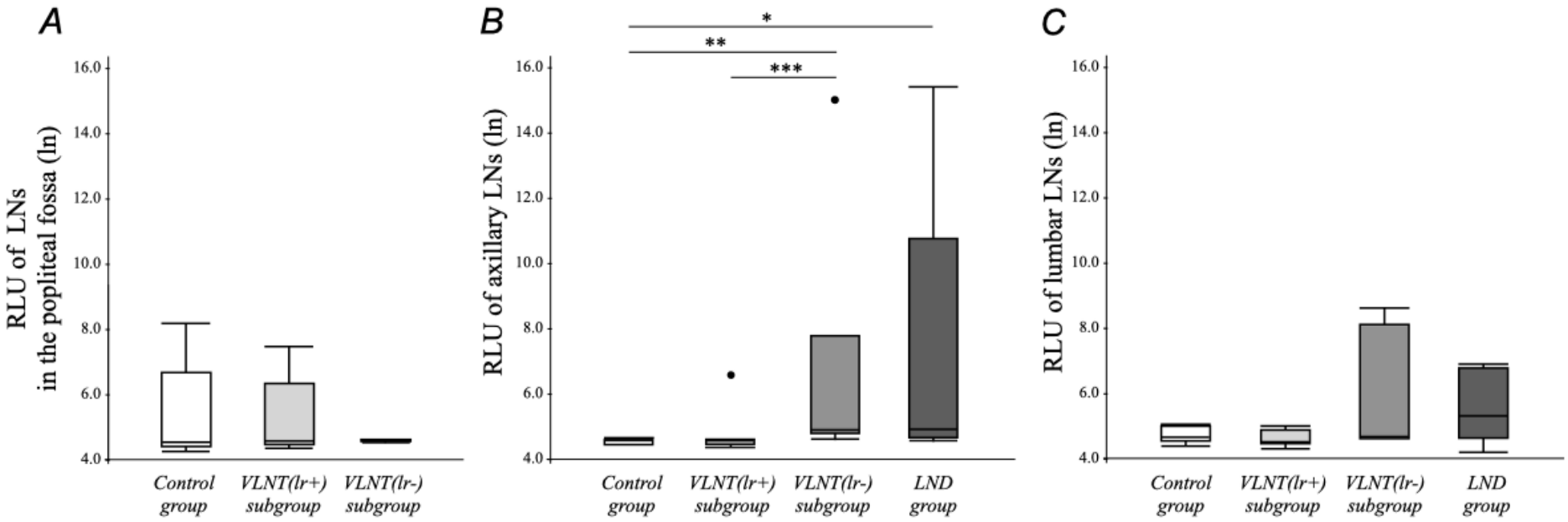
A
RLU of LNs in the popliteal fossa (ln)
16.0
14.0
12.0
10.0
8.0
6.0
4.0
Control group
VLNT(lr+) subgroup
VLNT(lr-) subgroup
B
RLU of axillary LNs (ln)
*
**
***
Control group
VLNT(lr+) subgroup
VLNT(lr-) subgroup
LND group
C
RLU of lumbar LNs (ln)
Control group
VLNT(lr+) subgroup
VLNT(lr-) subgroup
LND group

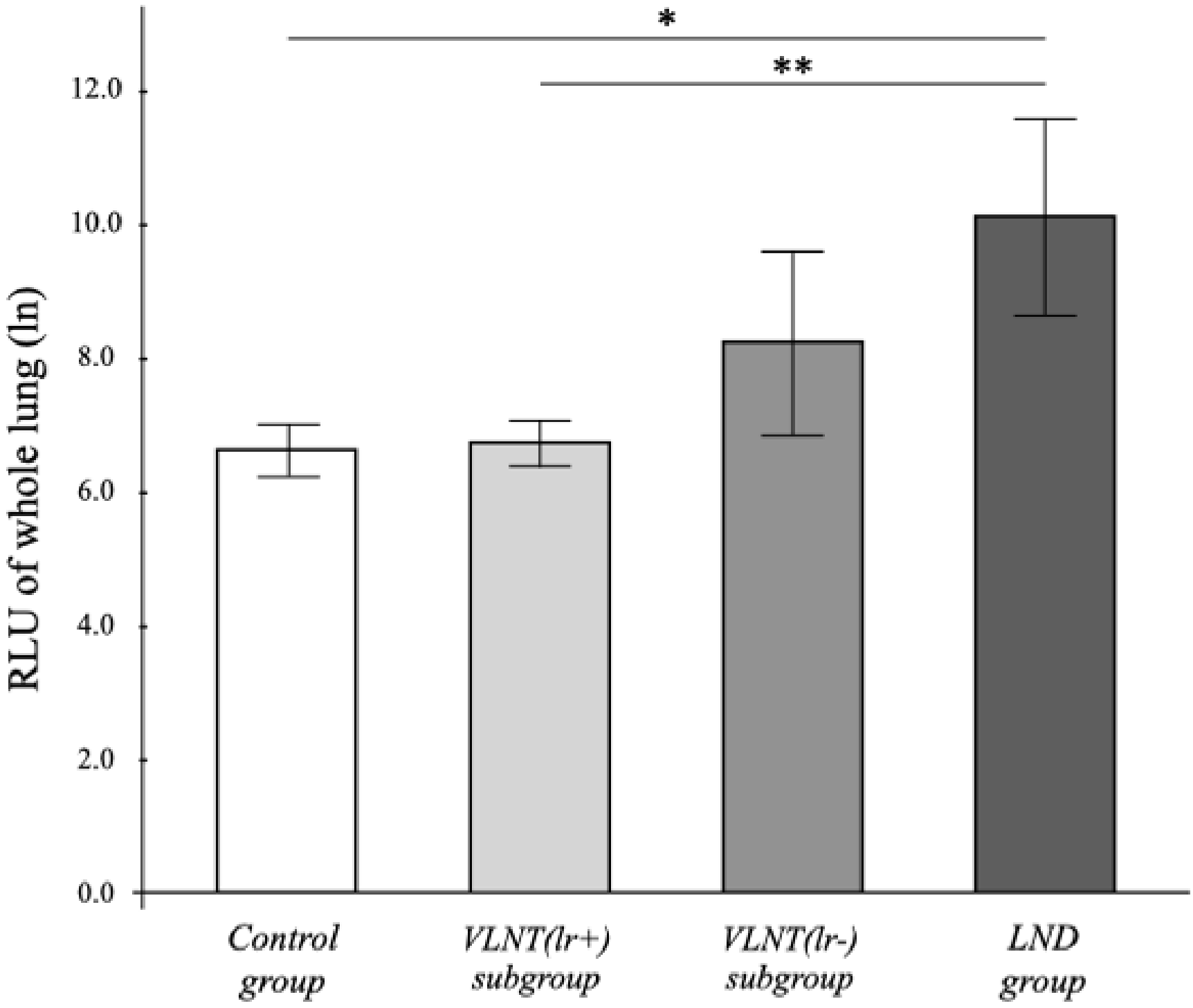
*
**
12.0
10.0
8.0
6.0
4.0
2.0
0.0
RLU of whole lung (ln)
Control group
VLNT(lr+) subgroup
VLNT(lr-) subgroup
LND group